STEP-UNROLLED DENOISING AUTOENCODERS FOR TEXT GENERATION

Nikolay Savinov* Junyoung Chung* Mikołaj Bińkowski*
Erich Elsen Aäron van den Oord
DeepMind, London, UK

ABSTRACT

In this paper we propose a new generative model of text, *Step-unrolled Denoising Autoencoder* (SUNDAE), that does not rely on autoregressive models. Similarly to denoising diffusion techniques, SUNDAE is repeatedly applied on a sequence of tokens, starting from random inputs and improving them each time until convergence. We present a simple new improvement operator that converges in fewer iterations than diffusion methods, while qualitatively producing better samples on natural language datasets. SUNDAE achieves state-of-the-art results (among non-autoregressive methods) on the WMT'14 English-to-German translation task and good qualitative results on unconditional language modeling on the Colossal Cleaned Common Crawl dataset and a dataset of Python code from GitHub. The non-autoregressive nature of SUNDAE opens up possibilities beyond left-to-right prompted generation, by filling in arbitrary blank patterns in a template.

1 Introduction

Autoregressive (AR) models have shown excellent results in generating text (e.g., GPT-3, Brown et al., 2020). However, while their training scales very well, sampling is prohibitively slow for many practical applications. Moreover, there are limitations to the kinds of conditioning AR models can seamlessly handle: the left-to-right restriction makes it hard to "fill in the gaps" in a partially written text draft. Even more importantly, this prohibits iterative refinement of complete text drafts to make them more self-consistent, which is a common task for human writers. Finally, AR models require network architectures to be causal, severely limiting the kinds of neural network architectures that can be used for text-modeling. All of these motivated the machine learning community to make extensive efforts to propose alternatives to AR models.

Machine translation (MT) was perhaps one of the first tasks where non-AR approaches were shown to seriously rival the AR-based state of the art: methods like CMLM (Ghazvininejad et al., 2019) and DisCo (Kasai et al., 2020) show promising results and their decoding speed is excellent compared to AR. However, while their performance is competitive, they are still behind the AR benchmark and actually require distillation of a larger AR model — without which, performance drops considerably.

Non-AR methods have proven hard to apply to the general unconditional language modeling (LM) task. When there is no conditioning, the multi-modality problem becomes paramount, as shown by Gu et al. (2017), which likely makes it problematic to use methods like CMLM and DisCo because their decoding mechanism is deterministic and does not model uncertainty. Yet, recently the community has seen promising results from non-AR models like Multinomial Diffusion (Hoogeboom et al., 2021) and D3PM (Austin et al., 2021). These methods optimize a lower bound (ELBO) on likelihoods and have shown negative log-likelihood (NLL) results approaching AR models on several benchmarks like text8 (Mahoney, 2011) and LM1B (Chelba et al., 2013). However, a major gap in NLL persists, and samples from those models lack coherence.

In this paper we propose a novel non-autoregressive method which shows state-of-the-art results in machine translation on WMT'14 EN→DE raw data (without distillation from AR) amongst non-AR methods and good qualitative results on unconditional language modeling on the Colossal Clean Common Crawl (C4) dataset (Raffel et al., 2019) and a dataset of Python code from GitHub. Our model operates as a time-homogeneous Markov Chain similar to that of Lee et al. (2018): conditioned on the corrupted data, it tries to approximate the original uncorrupted samples by a per-token

^{*}Shared first authorship.

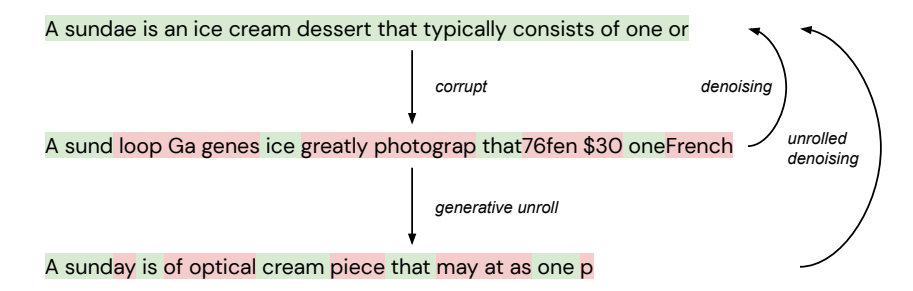


Figure 1: The difference between denoising and *unrolled denoising*. Original text (top) is randomly corrupted, producing a text (middle) where some tokens are original (green) and others are corrupted (red). This text is denoised by sampling from the generative model to produce another noisy text (bottom). While standard denoising autoencoders only learn a mapping from the middle text to the top text, *Step-unrolled Denoising Autoencoder* learns a mapping from bottom to top (including middle as a special case of zero unroll steps). This has an intuitive meaning: during generation time, the network will mostly (right after the first step) encounter texts like the bottom one, not like the middle one — so unrolls prepare the model during training for inputs it will get at generation time.

factorised distribution. During generation, we unroll the chain by sampling from the transition distribution and feeding samples back into the input. We propose a new training mechanism called *unrolled denoising*, which uses unrolls of the chain during training as well, and which we empirically show to be crucial for practical performance of the algorithm in ablation studies. This feature motivates the name for the model, *Step-unrolled Denoising Autoencoder* (SUNDAE). The difference between usual denoising and *unrolled denoising* is illustrated in Figure 1.

To summarize our contributions:

- We present SUNDAE, a new generative model of text that unrolls the denoising process during training.
- SUNDAE achieves state-of-the-art results on WMT'14 English-to-German translation task among non-AR methods.
- We demonstrate good qualitative results for unconditional generation and inpainting on Colossal Clean Common Crawl dataset and a dataset of Python code from GitHub.
- We carefully ablate and analyze the properties of the proposed method, and show that unrolls during training are crucial for the model's performance.

2 Method

We approach the problem of generative modelling of discrete sequences by bringing together the framework of denoising autoencoders and Markov chain models. In this section, we first discuss the definition of the generative model, and then describe the training process, which includes our main contribution, *unrolled denoising*.

For a fixed prior distribution p_0 on some space X consider a process $\mathbf{x}_t \sim f_{\theta}(\cdot|\mathbf{x}_{t-1})$, where f_{θ} is a parametric transition function. Then $\{\mathbf{x}_t\}_t$ is a time-homogeneous Markov chain, and transition t-steps ahead has the following form¹

$$p_t(\boldsymbol{x}_t|\boldsymbol{x}_0) = \sum_{\boldsymbol{x}_1, \boldsymbol{x}_2, \dots, \boldsymbol{x}_{t-1} \in X} \prod_{s=1}^t f_{\theta}(\boldsymbol{x}_s|\boldsymbol{x}_{s-1}).$$
 (1)

For a fixed number of steps T, the prior p_0 and decoder p_T together determine our model distribution $p_T(\mathbf{x}_T) = p_T(\mathbf{x}_T | \mathbf{x}_0) p_0(\mathbf{x}_0)$.

We assume $X = \{1, \dots, v\}^N$ to be the space of sequences of length N with values at all positions coming from a vocabulary of size v, and the prior p_0 to be uniform over X. Let p_{data} be a distribution of the data and assume that f_θ induces a conditional probability distribution $f_\theta(\cdot|\boldsymbol{x}')$ that can be

¹ for formal derivation, see Appendix A.

factorised into a conditionally-indepedent product as follows:

$$f_{\theta}(\boldsymbol{x}|\boldsymbol{x}') = f_{\theta}^{(1)}(\boldsymbol{x}^{(1)}|\boldsymbol{x}')f_{\theta}^{(2)}(\boldsymbol{x}^{(2)}|\boldsymbol{x}') \cdots f_{\theta}^{(N)}(\boldsymbol{x}^{(N)}|\boldsymbol{x}'), \quad \text{for } \boldsymbol{x}, \boldsymbol{x}' \in X.$$
 (2)

Note that although for t=1 the distribution $p_1(\cdot|\mathbf{x}_0)$ is limited by product structure (Eq. 2), the subsequent p_t s are not restricted in the same way, and after each step they belong to potentially more and more expressive family.

2.1 Training with Unrolled Denoising

Due to intractability of the likelihood of the model p_T as well as the computational requirements of optimising the whole chain $\{p_t\}_t$, we propose an efficient two-step training method which we term *unrolled denosing* and visualise in Figure 1. We consider a smaller number of steps than T that we intend to use at sampling, but to compensate for that, we unroll the chain starting from corrupted data samples, rather than the prior p_0 . This way, the model learns to denoise the samples it is likely to encounter during the full unroll used at sample time. While using a single step would resemble the training strategy of BERT (Devlin et al., 2018), using at least two steps is essential for the performance of our model.

Consider a *corruption* distribution $q(\mathbf{x}^c|\mathbf{x})$ that replaces a random proportion of tokens in a sentence \mathbf{x} with ones randomly sampled from a uniform distribution. Our objective is given by $L^{(1:2)} = \frac{1}{2} \left(L^{(1)} + L^{(2)} \right)$ where

$$L^{(t)}(\theta) := -\mathbb{E} \underset{\mathbf{x}_{0} \sim q(\cdot|\mathbf{x})}{\underset{\mathbf{x}_{1} \sim f_{\theta}(\cdot|\mathbf{x}_{0})}{\mathbf{x}_{1} \sim f_{\theta}(\cdot|\mathbf{x}_{t-2})}} [\log f_{\theta}(\mathbf{x}|\mathbf{x}_{t-1})], \tag{3}$$

i.e. the reconstruction loss of the chain after t steps, starting from a corrupted sample \mathbf{x}_0 . In Appendix A.1 we show that $L^{(t)}$ is an upper bound on the actual negative log-likelihood from the model distribution p_t :

$$\widetilde{L^{(t)}}(\theta) := -\mathbb{E} \underset{\mathbf{x}^c \sim q(\cdot|\mathbf{x})}{\mathbf{x}^{c} \sim q(\cdot|\mathbf{x})} [\log p_t(\mathbf{x}|\mathbf{x}^c)]. \tag{4}$$

Note that $L^{(T)}$ is the actual term we would like to minimise if p_T were tractable, and in fact is closely related to evidence lower bound (ELBO) via a fixed encoder $q(\mathbf{x}^c|\mathbf{x})$ (Appendix A.2). However, due to the inherent non-differentiable nature of discrete Markov chain models, optimisation of $\widetilde{L^{(T)}}$ would not only be costly, but also limit the gradient flow to the last step of the chain. We found instead that optimising several steps together without propagating the gradient through sampling is sufficient for obtaining good results. Averaging more $L^{(t)}$ terms can lead to minor improvements in performance (see Figure 4d in Appendix C), but it considerably slows down the training speed. We discuss these and other loss variants further in Section 3.1.

Since function f_{θ} is modelled as a neural network, the logarithm under expectation on the right hand side of Eq. 3 is obtained from predicted logits, thus we term $L^{(1)}(\theta)$ and $L^{(2)}(\theta)$ logits loss and unrolled logits loss, respectively.

Corruption function. To corrupt texts, we first sample a proportion of tokens uniformly from [0,1], randomly select positions according to this proportion and then change tokens at those positions to random tokens sampled uniformly from the vocabulary. This way, we want to ensure that samples seen at various steps during a generative unroll (including the first one, sampled from the uniform prior) are well-represented in corruptions applied during training. More details and relations to the forward diffusion process (Hoogeboom et al., 2021) are presented in Appendix A.3.

2.2 Sampling

At sampling time we follow the structure of the Markov process and sample sequentially $x_t \sim f_{\theta}(x_t|x_{t-1})$ for some fixed number of steps T, beginning from a random sequence x_0 (potentially starting with a prompt or a template for conditional generation). To control the speed of convergence, we propose three improved strategies which allow the use of a much smaller number of steps:

• Low-temperature sampling. For temperature τ and trained network f_{θ} we consider modified function f_{θ}^{τ} such that $\log f_{\theta}^{\tau}(\cdot|\boldsymbol{x}) \propto \frac{1}{\tau} \log f_{\theta}(\cdot|\boldsymbol{x})$. We found that sampling with temperatures lower than 1 leads to much faster convergence than with the original logits, and allowed generation of high-quality samples in a matter of 10-16 steps.

		Raw	BLEU	AR-distill	ed BLEU
Model	Steps (T)	EN→DE	DE→EN	EN→DE	DE→EN
AR Models					
Transformer Base (65M) (Vaswani et al., 2017) $(n=4)$	-	27.3	31.78*	-	-
Non-AR Models					
NAT (Gu et al., 2017) $(n=100)$	1	-	-	19.17	23.20
LVM-DAE (Lee et al., 2018)	-	-	-	21.54	25.43
NAT-REG (Wang et al., 2019) $(n=9)$	1	-	-	24.61	28.90
LV-NAR (Shu et al., 2020) $(n=50)$	1	11.8	-	25.10	-
NART w/ hints (Li et al., 2019) $(n=9)$	1	-	-	25.20	29.52
FlowSeq (Ma et al., 2019) $(n=30)$	1	23.64	28.29	25.31	30.68
ReorderNAT (Ran et al., 2019)	1	-	-	26.49	31.13
NART (Sun et al., 2019) $(n=19)$	1	-	-	26.80	30.04
CMLM (Ghazvininejad et al., 2019) + Mask-Predict ($n = 5$)	4	22.25	-	25.94	29.90
CMLM (Ghazvininejad et al., 2019) + Mask-Predict ($n = 5$)	10	24.61	-	27.03	30.53
DisCo (Kasai et al., 2020) + Mask-Predict $(n=5)$	4	-	-	25.83	30.15
DisCo (Kasai et al., 2020) + Mask-Predict $(n=5)$	10	-	-	27.06	30.89
DisCo (Kasai et al., 2020) + Easy-First ($n = 5$)	$4-5^{\dagger}$	24.8	-	27.34	31.31
NARLVM (Lee et al., 2020) $(n=25)$	4	-	-	27.40	-
JM-NAT (Guo et al., 2020) $(n=3)$	4	-	-	27.05	31.51
JM-NAT (Guo et al., 2020) $(n=3)$	10	-	-	27.69	32.54
SMART (Ghazvininejad et al., 2020) $(n=5)$	4	-	-	27.03	30.87
SMART (Ghazvininejad et al., 2020) $(n=5)$	10	-	-	27.65	31.27
Imputer (Saharia et al., 2020) $(n=1)$	4	24.7	-	28.0	31.0
Imputer (Saharia et al., 2020) $(n=1)$	8	25.2	-	28.2	31.3
SUNDAE (ours 63M)					
Deterministic $(n=16)$	4	25.01	29.53	28.33	32.25
Deterministic $(n=16)$	8	25.53	30.01	28.32	32.27
Deterministic $(n=16)$	10	25.54	30.11	28.32	32.27
Stochastic $(n=16)$	4	23.05	28.13	27.94	32.10
Stochastic $(n=16)$	8	26.08	30.48	28.23	32.33
Stochastic $(n=16)$	10	26.25	30.80	28.33	32.29
Stochastic $(n=16)$	16	26.24	30.76	28.46	32.30

Table 1: Test BLEU scores of AR and non-AR systems on the WMT'14 English-to-German (EN \rightarrow DE) and German-to-English (DE \rightarrow EN) translation tasks. The number of reranked candidates is denoted n. SUNDAE does not use an AR model for re-ranking. We highlight BLEU scores of the best non-AR systems in bold font. All the entries are ordered based on the EN \rightarrow DE BLEU score. *indicates the results of the Transformer baselines implemented by the authors of DisCo. †DisCo has a dynamic inference mode for which we report the average number of steps.

- Argmax-unrolled decoding. At the limit τ → 0 sampling with temperature reduces to deterministic argmax decoding where the most probable token is chosen at each step. Relatedly to our *unrolled logits* loss, we modify this strategy by resampling the low-certainty tokens in accordance with *unrolled logits*. This heuristic allowed further improvements to sampling speed while maintaining the high quality of the samples. We discuss it in detail in Section 3.1.
- **Updating fewer tokens**. In tasks where diversity is paramount (like unconditional text generation), we found that updating a random subset of tokens at each decoding step leads to faster convergence. This likely happens because independent sampling of all tokens might create uncoordinated changes which could take some time to fix in the subsequent steps. We use this strategy in Section 3.2.

3 EXPERIMENTS

3.1 MACHINE TRANSLATION

We first evaluate SUNDAE on Machine Translation (MT) benchmarks. We compare SUNDAE against AR and non-AR models in terms of the translation quality using BLEU (Papineni et al., 2002) as the metric. We demonstrate that without using techniques like sequence-level knowledge distillation (Kim & Rush, 2016), SUNDAE performs almost as well as the AR model and outperforms all other methods that do not rely on AR models.

Target Length Prediction. Unlike their AR counterparts, non-AR models do not explicitly learn to predict an end of sequence, but instead have been shown to benefit from auxiliary target length

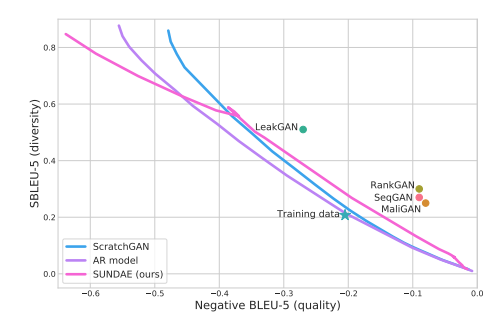
prediction (Lee et al., 2018; Ghazvininejad et al., 2019; Kasai et al., 2020). A common approach is to treat it as a classification task, predicting either the exact length or the difference between the source and target lengths. The decoding process has to commit to the predicted length, and often multiple length beams are used to get the best translation results. In our models, we use a separate network that receives source encodings as input and predicts corresponding target length. Target length embedding vector is prepended to source embeddings so that decoder can attend to it. During training, we use the reference target length, while at sampling, a predicted one, although the model does not need to fully commit to the predicted length like some previous non-AR models (Saharia et al., 2020). Note that the length classification loss does not affect the encoder parameters. Our models are also trained to predict the padding tokens at the end of the text. For more details, see Appendix B.

Experiment Settings. We conduct experiments on WMT'14 parallel corpora using $EN \leftrightarrow DE$ (4.5M pairs) and EN→FR (36M pairs) translation tasks. The raw texts are encoded using BPE (Sennrich et al., 2015) as the subword units, and we use the same preprocessed data as in Vaswani et al. (2017) for fair comparisons. We evaluate the performance by measuring BLEU (Papineni et al., 2002; Post, 2018) on the test split of each translation task². We use the encoder-decoder Transformer architecture for MT (Vaswani et al., 2017), but remove the causality masking in the decoder. There are 6 attention layers for both encoder and decoder, 8 attention heads, 512 model dimension and 2048 feedforward hidden dimension. The total number of parameters is 63M including the target length prediction module described in 3.1. We use dropout (p = 0.1) and label smoothing ($\epsilon = 0.1$) during training for all tasks, except for AR-distilled EN \rightarrow DE, where we found lower dropout (p=0.05) and no label smoothing produces better results on validation. The training batch size is 4096, and we use Adam (Kingma & Ba, 2014) with $\beta_1 = 0.9$, $\beta_2 = 0.999$, $\epsilon = 10^{-6}$ and weight decay of 0.1 (Loshchilov & Hutter, 2017). We warm up the learning rate from 10^{-7} to 10^{-4} in the first 5K steps and decay it to 10^{-5} using cosine annealing (Loshchilov & Hutter, 2016). Our models were trained for 10⁶ steps using 16 TPU accelerators using bfloat16 precision. We crop sequences that have more than 128 tokens (this occurs less than 0.2% in training data). Finally, we average the last 10 checkpoints to obtain a single model for the evaluation. All hyperparameter tuning is performed on a held-out validation set.

Decoding. We decode translations from SUNDAE using two different types of heuristic decoding methods in MT experiments. The decoding process always begins with an array of random integers sampled from the discrete uniform prior $y_0 \sim p_0$, while the encoder input - the source sentence remains the same throughout the process. The first decoding method is *low-temperature sampling*, where we iteratively sample $y_t \sim f_{\theta}^{\pi}(\cdot|y_{t-1})$ for T iterations (with the decoder output logits divided by τ , see Section 2.2), with $T \leq 16$ and $\tau \in [0.1, 0.6]$ determined based on the validation performance. The second method is argmax-unrolled decoding, which requires a smaller number of iterations compared to its stochastic counterpart. In argmax-unrolled decoding, we first compute the logits $\lambda_1 = f_{\theta}(\cdot|\mathbf{y}_0)$ of the initial sample array \mathbf{y}_0 and obtain the samples \mathbf{y}_1 , pass a tuple $(\mathbf{y}_1, \lambda_1)$ to the next iteration. At each step $t \ge 2$, the method finds top- ρ share of the tokens that are sorted by the log-probability in descending order (i.e. uncertain tokens) from λ_{t-1} , where $\rho \in [0.1, 0.6]$ is another hyperparameter searched for in the validation stage. We compute unrolled logits for those top- ρ tokens and then apply $\arg \max$ to obtain *unrolled tokens*. For the rest of the input tokens of y_{t-1} we compute logits once and obtain $\lambda_t = f_{\theta}(\cdot|y_{t-1})$ and then apply $\arg\max$ to obtain predicted tokens. Finally, we combine unrolled tokens for uncertain input positions with predicted tokens for remaining positions to obtain y_t , and the tuple (y_t, λ_t) is provided as the input to the next iteration. This procedure is repeated over a fixed number of iterations T. We always decode n samples in parallel and rerank them based on the model score. We show the relative speed gain of SUNDAE in Table 2, the Transformer base is used as the AR baseline, for which we perform incremental sampling by caching the previous attention states.

Baselines. We compare SUNDAE with Transformer base (Vaswani et al., 2017) as the AR baseline and several non-AR models including CMLM (Ghazvininejad et al., 2019) and DisCo (Kasai et al., 2020). The last two are both iterative non-AR models that share a substantial amount of common ground with SUNDAE. However, their best results come from the variants distilled from Transformer large (Vaswani et al., 2017), with only few test results available without distillation. As we aim to remove any kinds of dependencies on AR approaches, we would like to make a distinction

²Due to limited space, we report BLEU using SacreBLEU in Appendix G.



Steps (T)	Relative Speed Improvement
4	4.7x
8	2.6x
10	2.2x
16	1.4x

Figure 2: BLEU scores on EMNLP2017 News. Left is better, lower is better. Quality/variation is controlled by changing the temperature.

Table 2: Relative speed gain of SUNDAE over AR Transformer base (greedy decoding) on WMT'14 EN→DE validation set.

between raw, fully-non-AR models, and AR-distilled ones, i.e. those trained via distillation from large AR teachers (which typically perform better than the student models), or via AR reranking.

Results and Ablation Studies. In Table 1, we show test BLEU scores from SUNDAE and other baselines. On EN→DE, SUNDAE achieved 26.25 BLEU, and it performed the best among the raw non-AR models. To the best of our knowledge, SUNDAE achieved the closest result ($\triangle = 1.05$) to the score of Transformer base (Vaswani et al., 2017) without the aid of AR models.³ In the raw setting, argmax-unrolled decoding outperforms mask-predict (Ghazvininejad et al., 2019) and easyfirst (Kasai et al., 2020) by 0.74 BLEU when using the same amount of the worst-case compute budget. At T=8, SUNDAE performs better than Imputer (Saharia et al., 2020), which is a strong baseline that can generate high-quality translation within few (4-8) iterations. We discovered that as T increases, low-temperature sampling outperforms argmax-unrolled decoding, and at T=10, lowtemperature sampling outperforms Mask-Predict (Ghazvininejad et al., 2019) and Easy-First (Kasai et al., 2020) by 1.5 BLEU score. SUNDAE achieved 30.80 BLEU on DE EN, where there are not that many raw baselines to compare with. The difference between SUNDAE and the AR baseline on DE \rightarrow EN is 0.98. Finally, SUNDAE achieved 37.53 BLEU on EN \rightarrow FR at T=10, while the Transformer base (Vaswani et al., 2017) reported 38.1 BLEU on this task. Thus, SUNDAE without distillation is only 0.57 BLEU behind the standard AR baseline on EN \rightarrow FR. We present more details on EN \rightarrow FR scores in Table 7 in Appendix G.

While knowledge distillation was outside our main focus, we also report scores for AR-distilled SUNDAE.⁴ It again performed well, establishing new SotA on EN→DE translation among AR-distilled models, and being second only to JM-NAT (Guo et al., 2020) in DE→EN task.

We ablate the number of steps of *unrolled denoising* on EN \rightarrow DE test split. We observe that having at least one *unrolled denoising* step is crucial to obtain good performance in translation. With only the $L^{(1)}$ loss, SUNDAE achieves 11.19 BLEU, whereas using $L^{(1:2)}$, the score improves to 26.57 BLEU. Using $L^{(1:3)}$, i.e. averaging more *unrolled denoising* loss terms, did not improve the performance further, scoring 26.25 BLEU. The target length prediction also turned out to be an important component of our model: without it, the translation performance degrades on average by 2 BLEU score points on EN \rightarrow DE (see Appendix C). Finally, we qualitatively show how translation improves along the sampling steps by elimination of incoherent/repeated tokens in Table 5 in Appendix E.

3.2 TEXT GENERATION

Unconditional Text Generation (Qualitative). We train our method on a large high-quality publicly available Colossal Clean Common Crawl (C4) dataset (Raffel et al., 2019) to demonstrate samples. We tokenize the data using SentencePiece (Kudo & Richardson, 2018)⁵ with vocabulary size 32K and train on randomly cropped sequences of length 32. The network is the same as the Transformer decoder part for MT in Section 3.1 but is much larger — 335M parameters: 24 layers,

³As shown in Table 7 in Appendix G, allowing larger compute reduces the gap even further, to $\triangle = 0.73$.

⁴For distillation, we follow the protocol used by Saharia et al. (2020). Scores in Table 1 were obtained with distillation from Transformer–Big to allow direct comparisons with CMLM (Ghazvininejad et al., 2019) and SMART Ghazvininejad et al. (2020); for Transformer–Base–distilled scores see Table 6 in Appendix F.

⁵https://github.com/google/sentencepiece

Index	Type	Text
Prompt Seeing ***** for any visitor to a national park. While it is an exciting moment, a bear can ******		Seeing ****** for any visitor to a national park. While it is an exciting moment, a bear can *******
-	Completion	Seeing a big bear is a must for any visitor to a national park. While it is an exciting moment, a bear can be intimidating as it will come
2	Prompt	Seeing ****** for any visitor to a national park. While it is an exciting moment, a moose can ******
-	Completion	Seeing moose is a unique experience for any visitor to a national park. While it is an exciting moment, a moose can navigate its way through a forest

Table 3: Inpainting from our model trained on C4 (cherry-picked).

1024 embedding size, 4096 hidden size, 16 attention heads. Same as in the MT setup, we remove the causal mask since our model is non-autoregressive. We train up to 400K steps with Adam optimizer with batch size 4096 and use cosine annealing for scheduling the learning rate with minimum 10^{-5} , maximum $2*10^{-3}$ and linear warm-up of 10K steps from starting value of 10^{-7} .

The trained model is then used for unconditional sampling. Starting with 32 random tokens, we iteratively perform up to 1K steps from our model, stopping earlier if samples do not change anymore. To make convergence faster, we use temperature 0.8 and update only 30% of all tokens at each step, chosen randomly — as explained in Section 2.2. We show 10 non-cherry-picked samples from our model in Table 8 of Appendix H. Of those samples, all but one resemble reasonable internet texts.

Unconditional Text Generation (Quantitative). While C4 is one of the largest high-quality datasets publicly available, it does not have an established benchmark among non-AR methods. To quantitatively evaluate our algorithm, we train it on the EMNLP2017 News⁶ dataset, which has numerous text GAN baselines, including a strong ScratchGAN method (d'Autume et al., 2019). We also compare to several other baselines reported in (d'Autume et al., 2019; Caccia et al., 2020): SeqGAN (Yu et al., 2017), LeakGAN (Guo et al., 2017), RankGAN (Lin et al., 2017), MaliGAN (Che et al., 2017) and autoregressive (AR) language models.

We use the same architecture and optimizer as in qualitative experiments and train with batch size 1024 for 8K steps (chosen to achieve the lowest validation loss). We follow the same tokenization strategy as d'Autume et al. (2019), with vocabulary size of 5.7K and maximum length 52 tokens, padding shorter sequences to this maximum length. During sampling, we perform 1K steps and update all the tokens at each step (which we found beneficial for the chosen metrics). The quality/variation trade-off is controlled by changing the sampling temperature in the range [0.1, 2.0], using 60 values overall. For every temperature, we sample 10K texts for evaluating quality and another 10K texts for evaluating diversity, as done by d'Autume et al. (2019).

The results are shown in Figure 2. SUNDAE demonstrates good quality/variation trade-off, as measured by BLEU/self-BLEU metrics, outperforming 4 out of 5 GAN baselines, and competing with ScratchGAN and AR model. In the higher quality region, SUNDAE outperforms ScratchGAN, while in higher diversity region it slightly underperforms. The advantage of ScratchGAN in higher diversity region could be explained by its autoregressive decoding (it is a hybrid between AR and GAN). Interestingly, the curve for SUNDAE has a more complicated shape than the baselines — possibly because of its Markov Chain sampling, which can empirically exhibit something akin to "phase transitions". We show samples from SUNDAE in Table 9 of Appendix I.

Text In-painting. The non-autoregressive nature of our model opens up possibilities beyond left-to-right prompted generation, such as filling in arbitrary blank patterns in a template. In this section, we qualitatively investigate this new capability, using the C4-trained model described in previous sections, and another one, trained on a dataset of Python code from GitHub. All the architecture/training settings remain the same, except we train twice longer: up to 800K steps. Sampling settings are also the same, except we update all the tokens at each step as diversity is less of an issue with stronger conditioning. We construct the code dataset by extracting files ending in .py from open source GitHub repositories with licenses that are one of apache-2.0, mit, bsd-3-clause, bsd-2-clause, unlicense, cc0-1.0, isc, artistic-2.0. We perform document level de-duplication checking for exact matches.

For the C4 dataset, we present a model with a particular type of prompt <code>[CTX1][MSK1][CTX2][MSK2]</code>, where <code>[CTX]</code> stands for "context" and <code>[MSK]</code> for "masked", in Table 3, which shows how information can be "teleported" from arbitrary location to another arbitrary location, while taking into account bidirectional context. We change a species of the animal in <code>[CTX2]</code> and observe that the model actually uses the right word while in-painting

⁶http://www.statmt.org/wmt17/

Index	Type	Text
1	Prompt	def trunc_len(x, t): $*$ * * * * * * * * * * * * * return min(n, t)
	Completion	<pre>def trunc_len(x, t): n = len(x) return min(n, t)</pre>
Prompt		
	Completion	<pre>is_even = lambda x: x % 2 == 0 is_odd = lambda x: not is_even(x) # reuse</pre>

Table 4: Inpainting from our model trained on GitHub (cherry-picked).

[MSK1] and plausibly continues [MSK2] according to the species. This kind of task would be impossible to perform for an AR model: with left-to-right causality it would be unable to correctly guess the name of the animal, while with a right-to-left one it would have to start filling [MSK2] tokens first, so it would just ignore the conditioning. By contrast, our model succeeds in this task.

For GitHub Python data, we use two different kinds of prompts for our model in Table 4: <code>[CTX1][MSK1][CTX2]</code> and <code>[CTX1][MSK1][CTX2][MSK2][CTX3]</code>. In the first example, our model guesses that n should be the length of the input sequence and correctly in-paints <code>[MSK1]</code> region. This would again be impossible to do for AR models. Looking from left-to-right, it is impossible to guess that n will be the name of the length variable and t is meant to be a threshold. Looking from right-to-left, it is unclear what variables n and t represent and what is the function being computed. Only a bidirectional model can perform well in this task. In the second example, our model correctly follows the suggestion to reuse the function which it also has to in-paint.

Long-range unconditional generation (qualitative). Generating long texts unconditionally with non-autoregressive models is hard. In this section, we describe a technique which allows to largely overcome such diffuculties for SUNDAE.

The core idea is use a schedule for the number of updated tokens during the generation time. If the generation of N tokens is done over T steps, at time step t we update $\lfloor 2N*\min(t/T,1-t/T)\rfloor$ tokens, chosen randomly. This schedule has a triangular shape: first linear ramp-up and then linear decay. Empirically, we found the first part to be crucial. Intuitively, SUNDAE gradually builds stronger and stronger conditioning, until it is strong enough to update all tokens. Concurrently with our work, a similar schedule (without decay) was proposed in the MaskGIT paper (Chang et al., 2022) for image generation — suggesting the importance of the gradual ramp-up schedule for unconditional generation with autoencoders in general, beyond SUNDAE.

We train a longer-context SUNDAE on 256-token-length sequences of the C4 dataset. All other training details are identical to the settings for short-range unconditional generation described earlier, except that we use slightly smaller number of training steps $350 \mathrm{K}$ due to length-related overfitting increase. At generation time, we employ the update schedule described above (instead of always updating 30% tokens previously).

We show 5 selected samples from our model in Table 10 of Appendix K. Those samples resemble normal texts found on the internet and qualitatively have higher global coherence and grammatical correctness than samples from the discrete diffusion method (Austin et al., 2021).

4 RELATED WORK

In this section we provide an overview of generative models, focusing on applications in text domain.

4.1 AUTOREGRESSIVE MODELS

Early attempts to perform autoregressive modelling of text using neural networks began with Bengio et al. (2003); later Sutskever et al. (2011) extended this approach with RNNs. Since then, improvements in neural network architecture, such as the Transformer (Vaswani et al., 2017), and scaling up as with GPT-3 (Brown et al., 2020) dramatically improved the performance of AR models. While the architectures evolved, the loss function remained the same with minor modifications.

Insertion (Stern et al., 2019) and Levenshtein (Gu et al., 2019) Transformers are deviations from the standard paradigm of training and could potentially overcome some of AR problems. However, in the parallel decoding regime, they have to rely on AR distillation for obtaining competitive results.

4.2 Non-autoregressive models in general

Non-autoregressive models evolved in parallel with autoregressive ones but have so far struggled to address the same spectrum of tasks with the same quality as AR models.

Diffusion for generative models was originally introduced by Sohl-Dickstein et al. (2015). Recently Ho et al. (2020) proposed a different parametrization: instead of modeling one-step transitions, one could instead model $p(x_0|x_t)$ and later convert those to $p(x_{t-1}|x_t)$ by probabilistic reasoning. This was recently up-scaled for image modeling by Nichol & Dhariwal (2021) and extended to continuous time by Song et al. (2020). In terms of applications to text generation, two recent works addressed this: Hoogeboom et al. (2021) and Austin et al. (2021). Likelihoods obtained in those works are promising, but still behind AR and lacking sample quality as well.

Some diffusion works like Mittal et al. (2021) also approached modeling discrete sequences in another way: first encode sequences with a VAE into a continuous space and then apply continuous diffusion approaches commonly used for image generation.

Variational Autoencoders (VAEs) were proposed by Rezende et al. (2014) and Kingma & Welling (2013) as a likelihood-based extension of autoencoders. Application of such methods to text has been problematic empirically: as it was first noted in Bowman et al. (2015), good results come from using a strong AR decoder instead of a simple factorised one, but the latents are often ignored — which was named "posterior collapse problem". This problem was later tackled by Delta-VAEs (Razavi et al., 2019), with limited success in the text domain (Bosc & Vincent, 2020).

Normalising Flows (Dinh et al., 2014; Rezende & Mohamed, 2015; Dinh et al., 2016) are another prominent family of generative models, originally proposed for real-valued data and recently revisited for text generation by Hoogeboom et al. (2021). While conceptually interesting, the text samples of such methods lack in fidelity.

Generative Adversarial Networks (GANs) were originally introduced by Goodfellow et al. (2014) and remain one of the dominant methods for image generation. They were later adapted to text generation in Yu et al. (2017); Guo et al. (2017); Lin et al. (2017); Che et al. (2017). However, text generation with such methods is still a challenge, with a more recent ScratchGAN (d'Autume et al., 2019) showing relatively low-quality samples. At least part of the problem with applying GANs to text generation comes from non-differentiability of discrete text samples, which requires usage of zeroth order optimization methods.

Energy-Based models have a long history dating back to Hopfield (1982); Hinton (2002); LeCun et al. (2006); Ranzato et al. (2007). Recently, Deng et al. (2020) shows promising results for text.

4.3 Non-autoregressive models for machine translation

There have been many attempts to apply non-autoregressive methods to machine translation. Latent transformer (Kaiser et al., 2018) generated latent variables autoregressively and then decoded feed-forwardly. NAT (Gu et al., 2017) was the first to characterize a problem with non-autoregressive generation — "multi-modality". FlowSeq (Ma et al., 2019) applied Normalising Flows to machine translation. LVM-DAEs (Lee et al., 2018) are perhaps most related to our method, but these models do not have *unrolled denoising* and their decoding method is deterministic. The leading methods in this area are CMLM (Ghazvininejad et al., 2019) and DisCo (Kasai et al., 2020). While conceptually similar to LVM-DAEs (Lee et al., 2018), these works have introduced significant improvements to the training and decoding procedure, and, as a result, shown strong competition to AR methods. Both of them also do not have *unrolled denoising* and sampling like we do, but they are still powerful baselines. Later, there were attempts to combine CMLM with local AR (Kong et al., 2020). Perhaps the most related to our work is the SMART (Ghazvininejad et al., 2020) follow-up of the CMLM. However, this method is not probabilistic and it does not show unconditional generation capabilities. Finally, a recent line of work called Imputer (Chan et al., 2020; Saharia et al., 2020) achieves strong results in machine translation by aligning target to source via dynamic programming.

4.4 Denoising objective in general

With the advent of BERT (Devlin et al., 2018), the denoising objective became very popular for text representation learning. The original idea was later simplified in RoBERTa (Liu et al., 2019)

by removing the unnecessary next-sentence-prediction task and only retaining the denoising task (the cloze task). This is similar to our work, however, we do not apply masking to corrupt the input tokens, and instead only switch them to random ones. More importantly, RoBERTa does not use *unrolled denoising*. Another work, Electra (Clark et al., 2020a), deals with the same kind of corruption that we use, but instead of predicting the original token before the corruption, Electra predicts whether it was corrupted or not. Electric (Clark et al., 2020b) does not perform masking, but instead uses noise-contrastive loss to learn a representation of text. BART (Lewis et al., 2019) uses both BERT-style denoising and autoregressive modeling for learning representations. All of these methods were originally motivated by improving representation learning of text. There were a few attempts to heuristically decode models like BERT and turn them into text generative models such as in Wang & Cho (2019), however, samples from these models lack coherence.

5 CONCLUSION

In this paper we have proposed a novel non-autoregressive method that operates within the framework of denoising autoencoders and, crucially, unrolls the denoising process during training. *Unrolled denoising* allows us to achieve state-of-the art results in WMT'14 English-to-German translation task amongst non-AR methods (without distillation from large AR models) and good qualitative results in unconditional text modeling on C4 dataset. We have also qualitatively demonstrated new inpainting capabilities on C4 and GitHub Python data, which opens up new avenues for creative text editing where a human could more naturally collaborate with a machine on writing and even programming.

AUTHOR CONTRIBUTIONS

Nikolay Savinov came up with the idea of unrolled denoising, wrote the first prototype of unconditional generation, contributed to the machine translation codebase and co-led the project. Junyoung Chung wrote most of the machine translation codebase, came up with the length prediction conditioning, suggested argmax-unrolled decoding and co-led the project. Mikołaj Bińkowski came up with theoretical insights about our model, wrote most of the evaluation codebase, implemented model improvements and co-led the project. All three first authors contributed equally to writing the paper. Erich Elsen gave high-level scientific guidance, suggested text in-painting experiments and made substantial edits to the paper draft. Aäron van den Oord originally suggested to look into denoising generative models for text, gave high-level scientific guidance, proposed machine translation experiments and made substantial edits to the paper draft.

ACKNOWLEDGMENTS

We would like to thank Jean-Baptiste Alayrac and Miruna Pîslar for valuable discussions on the machine translation experiments, William Chan and Chitwan Saharia for sharing distilled translation datasets, Mihaela Rosca and Cyprien de Masson d'Autume for sharing text GAN evaluation code, Yujia Li and Jack Rae for sharing a dataset of Python code from GitHub, Sander Dieleman and Oriol Vinyals for in-depth feedback about our work, Jungo Kasai for responses to our questions about DisCo, Dani Yogatama for sharing knowledge on machine translation evaluation, and Jeff Donahue for feedback and discussions.

REFERENCES

Jacob Austin, Daniel Johnson, Jonathan Ho, Danny Tarlow, and Rianne van den Berg. Structured denoising diffusion models in discrete state-spaces. arXiv preprint arXiv:2107.03006, 2021.

Yoshua Bengio, Réjean Ducharme, Pascal Vincent, and Christian Janvin. A neural probabilistic language model. *The journal of machine learning research*, 3:1137–1155, 2003.

Tom Bosc and Pascal Vincent. Do sequence-to-sequence vaes learn global features of sentences? *arXiv preprint arXiv:2004.07683*, 2020.

Samuel R Bowman, Luke Vilnis, Oriol Vinyals, Andrew M Dai, Rafal Jozefowicz, and Samy Bengio. Generating sentences from a continuous space. *arXiv preprint arXiv:1511.06349*, 2015.

- Tom B Brown, Benjamin Mann, Nick Ryder, Melanie Subbiah, Jared Kaplan, Prafulla Dhariwal, Arvind Neelakantan, Pranav Shyam, Girish Sastry, Amanda Askell, et al. Language models are few-shot learners. *arXiv preprint arXiv:2005.14165*, 2020.
- Massimo Caccia, Lucas Caccia, William Fedus, Hugo Larochelle, Joelle Pineau, and Laurent Charlin. Language gans falling short. In 8th International Conference on Learning Representations, ICLR 2020, Addis Ababa, Ethiopia, April 26-30, 2020. OpenReview.net, 2020. URL https://openreview.net/forum?id=BJgza6VtPB.
- William Chan, Chitwan Saharia, Geoffrey Hinton, Mohammad Norouzi, and Navdeep Jaitly. Imputer: Sequence modelling via imputation and dynamic programming. In *International Conference on Machine Learning*, pp. 1403–1413. PMLR, 2020.
- Huiwen Chang, Han Zhang, Lu Jiang, Ce Liu, and William T Freeman. Maskgit: Masked generative image transformer. *arXiv preprint arXiv:2202.04200*, 2022.
- Tong Che, Yanran Li, Ruixiang Zhang, R Devon Hjelm, Wenjie Li, Yangqiu Song, and Yoshua Bengio. Maximum-likelihood augmented discrete generative adversarial networks. arXiv preprint arXiv:1702.07983, 2017.
- Ciprian Chelba, Tomas Mikolov, Mike Schuster, Qi Ge, Thorsten Brants, and Phillipp Koehn. One billion word benchmark for measuring progress in statistical language modeling. *CoRR*, abs/1312.3005, 2013. URL http://arxiv.org/abs/1312.3005.
- Kevin Clark, Minh-Thang Luong, Quoc V Le, and Christopher D Manning. Electra: Pre-training text encoders as discriminators rather than generators. *arXiv preprint arXiv:2003.10555*, 2020a.
- Kevin Clark, Minh-Thang Luong, Quoc V Le, and Christopher D Manning. Pre-training transformers as energy-based cloze models. *arXiv* preprint arXiv:2012.08561, 2020b.
- Cyprien de Masson d'Autume, Mihaela Rosca, Jack Rae, and Shakir Mohamed. Training language gans from scratch. *arXiv preprint arXiv:1905.09922*, 2019.
- Yuntian Deng, Anton Bakhtin, Myle Ott, Arthur Szlam, and Marc'Aurelio Ranzato. Residual energy-based models for text generation. *arXiv preprint arXiv:2004.11714*, 2020.
- Jacob Devlin, Ming-Wei Chang, Kenton Lee, and Kristina Toutanova. Bert: Pre-training of deep bidirectional transformers for language understanding. *arXiv preprint arXiv:1810.04805*, 2018.
- Laurent Dinh, David Krueger, and Yoshua Bengio. Nice: Non-linear independent components estimation. arXiv preprint arXiv:1410.8516, 2014.
- Laurent Dinh, Jascha Sohl-Dickstein, and Samy Bengio. Density estimation using real nvp. *arXiv* preprint arXiv:1605.08803, 2016.
- Marjan Ghazvininejad, Omer Levy, Yinhan Liu, and Luke Zettlemoyer. Mask-predict: Parallel decoding of conditional masked language models. *arXiv preprint arXiv:1904.09324*, 2019.
- Marjan Ghazvininejad, Omer Levy, and Luke Zettlemoyer. Semi-autoregressive training improves mask-predict decoding. *arXiv* preprint arXiv:2001.08785, 2020.
- Ian Goodfellow, Jean Pouget-Abadie, Mehdi Mirza, Bing Xu, David Warde-Farley, Sherjil Ozair, Aaron Courville, and Yoshua Bengio. Generative adversarial nets. Advances in neural information processing systems, 27, 2014.
- Jiatao Gu, James Bradbury, Caiming Xiong, Victor OK Li, and Richard Socher. Non-autoregressive neural machine translation. *arXiv preprint arXiv:1711.02281*, 2017.
- Jiatao Gu, Changhan Wang, and Jake Zhao. Levenshtein transformer. *arXiv preprint arXiv:1905.11006*, 2019.
- Jiaxian Guo, Sidi Lu, Han Cai, Weinan Zhang, Yong Yu, and Jun Wang. Long text generation via adversarial training with leaked information. arxiv e-prints, art. arXiv preprint arXiv:1709.08624, 2017.

- Junliang Guo, Linli Xu, and Enhong Chen. Jointly masked sequence-to-sequence model for non-autoregressive neural machine translation. In *Proceedings of the 58th Annual Meeting of the Association for Computational Linguistics*, pp. 376–385, 2020.
- Geoffrey E Hinton. Training products of experts by minimizing contrastive divergence. *Neural computation*, 14(8):1771–1800, 2002.
- Jonathan Ho, Ajay Jain, and Pieter Abbeel. Denoising diffusion probabilistic models. *arXiv* preprint *arXiv*:2006.11239, 2020.
- Emiel Hoogeboom, Didrik Nielsen, Priyank Jaini, Patrick Forré, and Max Welling. Argmax flows and multinomial diffusion: Towards non-autoregressive language models. arXiv preprint arXiv:2102.05379, 2021.
- John J Hopfield. Neural networks and physical systems with emergent collective computational abilities. *Proceedings of the national academy of sciences*, 79(8):2554–2558, 1982.
- Lukasz Kaiser, Samy Bengio, Aurko Roy, Ashish Vaswani, Niki Parmar, Jakob Uszkoreit, and Noam Shazeer. Fast decoding in sequence models using discrete latent variables. In *International Conference on Machine Learning*, pp. 2390–2399. PMLR, 2018.
- Jungo Kasai, James Cross, Marjan Ghazvininejad, and Jiatao Gu. Non-autoregressive machine translation with disentangled context transformer. In *International Conference on Machine Learning*, pp. 5144–5155. PMLR, 2020.
- Yoon Kim and Alexander M Rush. Sequence-level knowledge distillation. arXiv preprint arXiv:1606.07947, 2016.
- Diederik P Kingma and Jimmy Ba. Adam: A method for stochastic optimization. arXiv preprint arXiv:1412.6980, 2014.
- Diederik P Kingma and Max Welling. Auto-encoding variational bayes. *arXiv preprint* arXiv:1312.6114, 2013.
- Xiang Kong, Zhisong Zhang, and Eduard Hovy. Incorporating a local translation mechanism into non-autoregressive translation. *arXiv preprint arXiv:2011.06132*, 2020.
- Taku Kudo and John Richardson. Sentencepiece: A simple and language independent subword tokenizer and detokenizer for neural text processing. *arXiv* preprint arXiv:1808.06226, 2018.
- Yann LeCun, Sumit Chopra, Raia Hadsell, M Ranzato, and F Huang. A tutorial on energy-based learning. *Predicting structured data*, 1(0), 2006.
- Jason Lee, Elman Mansimov, and Kyunghyun Cho. Deterministic non-autoregressive neural sequence modeling by iterative refinement. *arXiv preprint arXiv:1802.06901*, 2018.
- Jason Lee, Raphael Shu, and Kyunghyun Cho. Iterative refinement in the continuous space for non-autoregressive neural machine translation. *arXiv* preprint arXiv:2009.07177, 2020.
- Mike Lewis, Yinhan Liu, Naman Goyal, Marjan Ghazvininejad, Abdelrahman Mohamed, Omer Levy, Ves Stoyanov, and Luke Zettlemoyer. Bart: Denoising sequence-to-sequence pretraining for natural language generation, translation, and comprehension. *arXiv* preprint *arXiv*:1910.13461, 2019.
- Zhuohan Li, Zi Lin, Di He, Fei Tian, Tao Qin, Liwei Wang, and Tie-Yan Liu. Hint-based training for non-autoregressive machine translation. *arXiv preprint arXiv:1909.06708*, 2019.
- Kevin Lin, Dianqi Li, Xiaodong He, Zhengyou Zhang, and Ming-Ting Sun. Adversarial ranking for language generation. *arXiv preprint arXiv:1705.11001*, 2017.
- Yinhan Liu, Myle Ott, Naman Goyal, Jingfei Du, Mandar Joshi, Danqi Chen, Omer Levy, Mike Lewis, Luke Zettlemoyer, and Veselin Stoyanov. Roberta: A robustly optimized bert pretraining approach. *arXiv preprint arXiv:1907.11692*, 2019.

- Ilya Loshchilov and Frank Hutter. Sgdr: Stochastic gradient descent with warm restarts. *arXiv* preprint arXiv:1608.03983, 2016.
- Ilya Loshchilov and Frank Hutter. Decoupled weight decay regularization. *arXiv preprint* arXiv:1711.05101, 2017.
- Xuezhe Ma, Chunting Zhou, Xian Li, Graham Neubig, and Eduard Hovy. Flowseq: Non-autoregressive conditional sequence generation with generative flow. *arXiv preprint arXiv:1909.02480*, 2019.
- Matt Mahoney. Text 8 dataset. http://mattmahoney.net/dc/textdata, 2011. Accessed: 2021-09-29.
- Gautam Mittal, Jesse Engel, Curtis Hawthorne, and Ian Simon. Symbolic music generation with diffusion models. *arXiv preprint arXiv:2103.16091*, 2021.
- Alex Nichol and Prafulla Dhariwal. Improved denoising diffusion probabilistic models. *arXiv* preprint arXiv:2102.09672, 2021.
- Kishore Papineni, Salim Roukos, Todd Ward, and Wei-Jing Zhu. Bleu: a method for automatic evaluation of machine translation. In *Proceedings of the 40th annual meeting of the Association for Computational Linguistics*, pp. 311–318, 2002.
- Matt Post. A call for clarity in reporting bleu scores. arXiv preprint arXiv:1804.08771, 2018.
- Colin Raffel, Noam Shazeer, Adam Roberts, Katherine Lee, Sharan Narang, Michael Matena, Yanqi Zhou, Wei Li, and Peter J. Liu. Exploring the limits of transfer learning with a unified text-to-text transformer. *arXiv e-prints*, 2019.
- Qiu Ran, Yankai Lin, Peng Li, and Jie Zhou. Guiding non-autoregressive neural machine translation decoding with reordering information. *arXiv preprint arXiv:1911.02215*, 2019.
- Marc'Aurelio Ranzato, Y-Lan Boureau, Sumit Chopra, and Yann LeCun. A unified energy-based framework for unsupervised learning. In Artificial Intelligence and Statistics, pp. 371–379. PMLR, 2007.
- Ali Razavi, Aäron van den Oord, Ben Poole, and Oriol Vinyals. Preventing posterior collapse with delta-vaes. *arXiv preprint arXiv:1901.03416*, 2019.
- Danilo Rezende and Shakir Mohamed. Variational inference with normalizing flows. In *International conference on machine learning*, pp. 1530–1538. PMLR, 2015.
- Danilo Jimenez Rezende, Shakir Mohamed, and Daan Wierstra. Stochastic backpropagation and approximate inference in deep generative models. In *International conference on machine learning*, pp. 1278–1286. PMLR, 2014.
- Chitwan Saharia, William Chan, Saurabh Saxena, and Mohammad Norouzi. Non-autoregressive machine translation with latent alignments. *arXiv preprint arXiv:2004.07437*, 2020.
- Rico Sennrich, Barry Haddow, and Alexandra Birch. Neural machine translation of rare words with subword units. *arXiv preprint arXiv:1508.07909*, 2015.
- Raphael Shu, Jason Lee, Hideki Nakayama, and Kyunghyun Cho. Latent-variable non-autoregressive neural machine translation with deterministic inference using a delta posterior. In *Proceedings of the AAAI Conference on Artificial Intelligence*, volume 34, pp. 8846–8853, 2020.
- Jascha Sohl-Dickstein, Eric Weiss, Niru Maheswaranathan, and Surya Ganguli. Deep unsupervised learning using nonequilibrium thermodynamics. In *International Conference on Machine Learn-ing*, pp. 2256–2265. PMLR, 2015.
- Yang Song, Jascha Sohl-Dickstein, Diederik P Kingma, Abhishek Kumar, Stefano Ermon, and Ben Poole. Score-based generative modeling through stochastic differential equations. *arXiv* preprint *arXiv*:2011.13456, 2020.

- Mitchell Stern, William Chan, Jamie Kiros, and Jakob Uszkoreit. Insertion transformer: Flexible sequence generation via insertion operations. In *International Conference on Machine Learning*, pp. 5976–5985. PMLR, 2019.
- Zhiqing Sun, Zhuohan Li, Haoqing Wang, Zi Lin, Di He, and Zhi-Hong Deng. Fast structured decoding for sequence models. *arXiv* preprint arXiv:1910.11555, 2019.
- Ilya Sutskever, James Martens, and Geoffrey E Hinton. Generating text with recurrent neural networks. In *ICML*, 2011.
- Ashish Vaswani, Noam Shazeer, Niki Parmar, Jakob Uszkoreit, Llion Jones, Aidan N Gomez, Łukasz Kaiser, and Illia Polosukhin. Attention is all you need. In *Advances in neural information processing systems*, pp. 5998–6008, 2017.
- Alex Wang and Kyunghyun Cho. Bert has a mouth, and it must speak: Bert as a markov random field language model. *arXiv preprint arXiv:1902.04094*, 2019.
- Yiren Wang, Fei Tian, Di He, Tao Qin, ChengXiang Zhai, and Tie-Yan Liu. Non-autoregressive machine translation with auxiliary regularization. In *Proceedings of the AAAI Conference on Artificial Intelligence*, volume 33, pp. 5377–5384, 2019.
- Lantao Yu, Weinan Zhang, Jun Wang, and Yong Yu. Sequence generative adversarial nets with policy gradient. In *Proceedings of the AAAI conference on artificial intelligence*, volume 31, 2017.

A METHOD DETAILS

Using Markov property and the form of $p_t = f_{\theta}(\cdot|\mathbf{x}_{t-1})$, for any t > 0 we obtain

$$p_t(\mathbf{x}_t|\mathbf{x}_0) = \sum_{\boldsymbol{x}_{t-1} \in X} p_{t-1}(\boldsymbol{x}_{t-1}|\mathbf{x}_0) f_{\theta}(\mathbf{x}_t|\boldsymbol{x}_{t-1})$$
(5)

$$= \mathbb{E}_{\mathbf{x}_{t-1} \sim p_{t-1}(\cdot|\mathbf{x}_0)} f_{\theta}(\mathbf{x}_t|\mathbf{x}_{t-1}). \tag{6}$$

By induction, we can keep unrolling the chain for all steps $s=t-1,t-2,\ldots,1$, eventually obtaining

$$p_{t}(\boldsymbol{x}_{t}|\boldsymbol{x}_{0}) = \sum_{\substack{\boldsymbol{x}_{1}, \dots, \boldsymbol{x}_{t-1} \\ \in X}} \prod_{s=1}^{t} f_{\theta}(\boldsymbol{x}_{s}|\boldsymbol{x}_{s-1})$$

$$= \mathbb{E}_{\substack{\boldsymbol{x}_{1} \sim p_{1}(\cdot|\boldsymbol{x}_{0}) \\ \dots \\ \boldsymbol{x}_{t-1} \sim p_{t-1}(\cdot|\boldsymbol{x}_{t-2})}} [f_{\theta}(\boldsymbol{x}_{t}|\boldsymbol{x}_{t-1})], \qquad (7)$$

which proves the from of the model distribution (Eq. 1).

A.1 UPPER BOUND ON THE LOSS.

Using Jensen's inequality we can swap log and expectation in Eq. 7 to obtain

$$-\log p_{t}(\mathbf{x}|\mathbf{x}_{0}) \leq -\mathbb{E}_{\substack{\mathbf{x}_{1} \sim p_{1}(\cdot|\mathbf{x}_{0}) \\ \dots \\ \mathbf{x}_{t-1} \sim p(\cdot|\mathbf{x}_{t-2})}} \left[\log f_{\theta}(\mathbf{x}|\mathbf{x}_{t-1})\right], \tag{8}$$

hence

$$\widetilde{L^{(t)}}(\theta) = -\mathbb{E} \underset{\mathbf{x}_0 \sim q(\cdot|\mathbf{x})}{\mathbf{x}_{-2}(\mathbf{x})} \left[\log p_t(\mathbf{x}|\mathbf{x}_0) \right] \le -\mathbb{E} \underset{\mathbf{x}_1 \sim f_{\theta}(\cdot|\mathbf{x}_0)}{\mathbf{x}_{-2}(\mathbf{x})} \left[\log f_{\theta}(\mathbf{x}|\mathbf{x}_{t-1}) \right] = L^{(t)}(\theta). \tag{9}$$

$$\mathbf{x}_{t-1} \sim \widetilde{f_{\theta}}(\cdot|\mathbf{x}_{t-2})$$

A.2 RELATION TO VAE

Variational Autoencoders (Kingma & Welling, 2013; Rezende et al., 2014) optimise the expected evidence lower bound (ELBO) on the marginal likelihood

$$\log p(\mathbf{x}) \ge -D_{\mathrm{KL}}(q(\mathbf{z}|\mathbf{x})||p_0(\mathbf{z})) + \mathbb{E}_{\mathbf{z} \sim q(\cdot|\mathbf{x})} \left[\log p(\mathbf{x}|\mathbf{z})\right], \tag{10}$$

with respect to parameters of both the variational distribution q and generative distribution p, where p_0 remains the prior for for the latent variables. Denosing autoencoders limit the optimisation to the second term, assuming a fixed encoder q, which is also the case with SUNDAE: identifying encoder with our corruption distribution and generative distribution p with the distribution of our chain at the last step p_T , expected ELBO becomes

$$\mathbb{E}_{\mathbf{x} \sim p_{\text{data}}}[\log p_T(\mathbf{x})] \ge -\mathbb{E}_{\mathbf{x} \sim p_{\text{data}}}[D_{\text{KL}}(q(\mathbf{z}|\mathbf{x})||p_0(\mathbf{z}))] + \mathbb{E}_{\substack{\mathbf{x} \sim p_{\text{data}} \\ \mathbf{x}^c \sim q(\cdot|\mathbf{x})}}[\log p_t(\mathbf{x}|\mathbf{x}^c)]$$

$$\ge -\mathbb{E}_{\mathbf{x} \sim p_{\text{data}}}[D_{\text{KL}}(q(\mathbf{z}|\mathbf{x})||p_0(\mathbf{z}))] - L^{(T)}(\theta). \tag{11}$$

where the second inequality is a consequence of the upper bound 3. Hence, minimizing $L^{(T)}$ would lead to maximisation of the lower bound on the model likelihood.

A.3 CORRUPTION FUNCTION

Our corruption function is obtained in stages:

- sample uniform expected corruption proportion $\alpha \sim \mathcal{U}([0,1])$,
- sample Bernoulli mask, independently for each token $m \sim (\text{Bernoulli}(\alpha))^N$,
- sample noise $\eta \sim (\mathcal{U}(\{1, 2, \dots, v\})^N,$

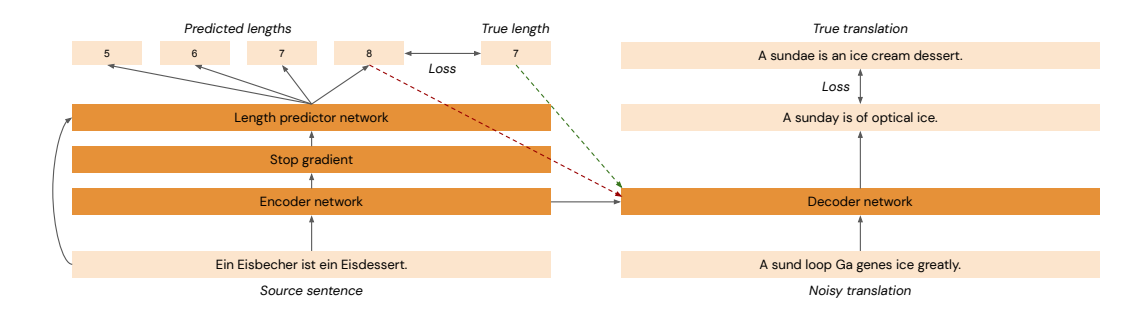


Figure 3: Overview of target length prediction. During SUNDAE training, we simultaneously train the length predictor with cross-entropy loss and give ground-truth target length as input to the decoder (green dashed arrow), thus teacher-forcing it. During sampling, we give the most likely target length prediction from the network to the decoder (red dashed arrow).

• compute corruption $x^c = c_{\alpha,m,\eta}(x) = (1 - m) \cdot x + m \cdot \eta$ (with multiplications taken element-wise).

The distribution $p^c(\cdot|\mathbf{x})p_{\text{data}}(\mathbf{x})$ obtained in this process covers the entire input space X, with probability skewed towards samples whose parts come from p_{data} . Note that except for corruption proportion, all steps are independent for all individual tokens. Given α , $p^{c_{\alpha}}(\mathbf{y}|\mathbf{x})$ can be factorised as

$$\prod_n p^{c_\alpha}(\boldsymbol{y}^{(n)}|\boldsymbol{x}^{(n)}) = \prod_n h(\boldsymbol{y}^{(n)})^T \boldsymbol{Q}_\alpha h(\boldsymbol{x}^{(n)}),$$

where $Q_{\alpha} = \alpha I + (1 - \alpha)V$ is a transition matrix, V is a $v \times v$ matrix with all entries equal to $\frac{1}{v}$, and h(a) denotes one-hot vector representation of $a \in \{1, 2, \dots, v\}$. In this context, corruption with rate α corresponds to a *multinomial-diffusion forward process* with probability α of remaining in the same state, as proposed by (Hoogeboom et al., 2021).

B DETAILS OF TARGET LENGTH PREDICTION

We provide a simplified high-level overview of the target length predictor in Figure 3. In the rest of this section we focus on implementation details.

The target length prediction module consists of 6 residual blocks. The length prediction module takes the source encodings $h_x = encoder(x)$ as the input, where x is a sequence of source tokens. We first project h_x into a vector $v_x \in \mathbb{R}^{d_{LP}}$, where $d_{LP} = 128$ is the hidden size of the target length prediction module. We add a source length embedding vector $v_{len} = S_{(N_{source} \times d_{LP})}(l_x)$ to v_x and obtain the final encoder state representation $v_x' = v_x + v_{len}$, where l_x is the number of the source tokens, and $N_{source} = 128$ is the maximum number of the source tokens. The target length prediction module then takes v_x as the input and predicts the (downsampled) target length \tilde{l}_d . We found beneficial downsampling the target lengths for the length prediction by a factor of 2, i.e. $l_d = \lceil l/2 \rceil$ as compared to exact prediction of l; since the maximum number of target tokens is N=128, the maximum size of the outcome of length prediction is $N_d=64$.

We prepend an embedding $h_{len} \in \mathbb{R}^{d_{enc}}$ of target length to the source encodings $h_x \in \mathbb{R}^{N_{source} \times d_{enc}}$ for each source example x and allow the decoder to attend to it $(d_{enc}$ here denotes the dimensionality of the encoder). h_{len} is obtained by applying an embedding matrix $V_{(N_d \times d_{enc})}$ to ground truth (downsampled) length l_d at training time, or to predicted one \tilde{l}_d during sampling. Note that optimisation of the length classification loss does not affect the encoder parameters.

C EFFECTS OF TARGET LENGTH PREDICTION

It is shown empirically that the length of the translated results can affect BLEU score. Approximate search methods such as beam search usually incorporate a length normalization term in order to prevent the search algorithm to prefer shorter sentences. This is due to the fact that the scoring function

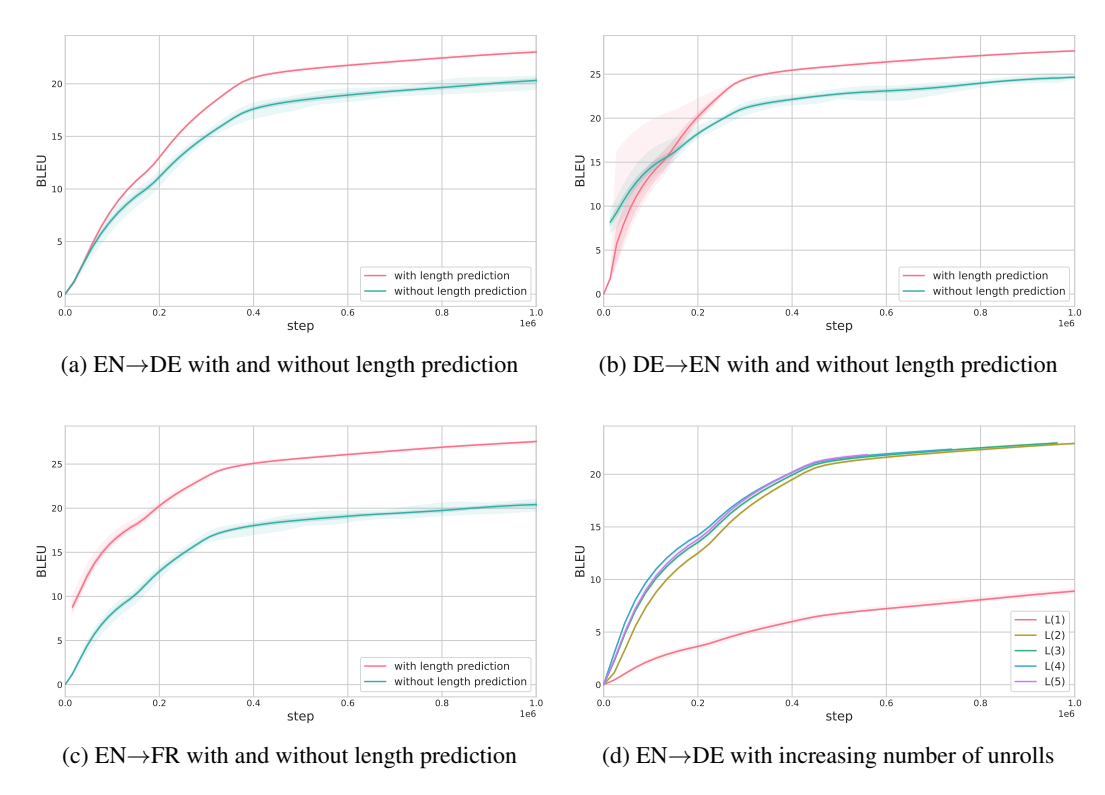


Figure 4: Validation BLEU curves during training with and without target length prediction on WMT'14 EN \rightarrow DE, DE \rightarrow EN and EN \rightarrow FR tasks shown in Figure 4a, 4b and 4c, respectively. Figure 4d shows the effect of *unrolled denoising* terms on translation quality, here $L(k) = L^{(1:k)}$. All models are trained with a batch size of 256 using 20 different random seeds to display uncertainty.

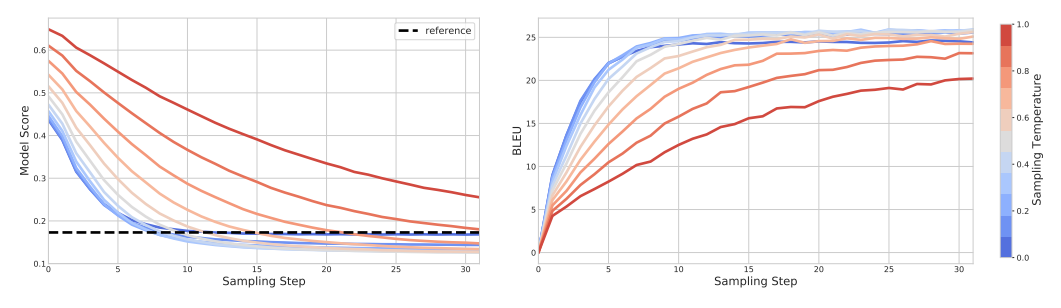
Source	Ich habe dort Dinge gesehen, aus denen ich gestärkt hervorgegangen bin.
Initialization Step 1 Step 2 Step 3 Step 4	ThirVerschlMarta moderatopposed frameworks solidierweitert [] I saw things there that which I I stronger I saw things there from which I me stronger I saw things there from which I emerged stronger. I saw things there from which I emerged stronger.
Reference	I saw some things there and came out stronger.

Table 5: German-to-English translation process. Since initialization is quite long, we substitute the trailing tokens with [...]. Tokens changed from previous step are highlighted in gray. The process converges after 3 steps, while AR would take 10 steps (one for each token in the translation).

is usually chosen as the likelihood modelled by the translation system, and beams containing shorter sequences tend to score higher likelihoods. In non-AR models, the end of sequence is not explicitly learned by the models, thus they can benefit by knowing the target sequence length in advance to generating the translation. However, the length of the target sequence cannot be known at inference time, therefore, a model should predict it instead. We show how BLEU scores can differ in WMT'14 translation tasks with and without the target length prediction in Figure 4a-4c.

D EFFECTS OF UNROLLED LOGITS LOSSES

We show how varying the number of unrolled logits can affect the MT performance in Figure 4d.



- (a) Model score evolution throughout sampling.
- (b) BLEU evolution throughout sampling.

Figure 5: Model score (left) and BLEU (right) evolution throughout sampling for various temperatures. The reference score on the left hand side denotes the model score obtained for ground truth inputs. Overall, medium-low temperatures give the best results.

E TRANSLATION ANALYSIS

We show how our algorithm works step-by-step for translation in Table 5. It is interesting to observe how the multimodality problem (Gu et al., 2017) gets resolved with more steps. Multimodality usually manifests in repeated tokens in translation, which intrinsically comes from inability to coordinate decisions when independently sampling multiple tokens at once. However, after a few steps all repetitions are corrected, because the model conditions on the previous step and hence can better coordinate further changes.

Figure 5 shows how the model and the BLEU scores evolve during sampling for various temperatures. The model score here refers to the cross-entropy between translation and model logits produced by giving this translation as the input. While for very low temperatures the scores initially improve faster, they are eventually outperformed by scores for higher temperatures, possibly due to low diversity induced by near-deterministic sampling. For very high temperatures, on the other hand, the scores improve slowly, and hence using such temperatures is rather impractical.

F DISTILLATION SCORES OBTAINED WITH TRANSFORMER-BASE

In Table 6 we also present results for SUNDAE trained on data distilled from autoregressive Transformer-Base model, which allows direct comparison with similarly obtained Imputer scores (Saharia et al., 2020). The results show that SUNDAE noticeably outperforms Imputer at 8 steps for both $EN \rightarrow DE$ and $DE \rightarrow EN$ language pairs.

		AR-distilled BLEU		
Model	Steps (T)	$EN \rightarrow DE$	$DE \rightarrow EN$	
Imputer (Saharia et al., 2020) $(n=1)$	4	27.9	30.9	
Imputer (Saharia et al., 2020) $(n=1)$	8	27.9	31.1	
SUNDAE (63M)				
Deterministic $(n=16)$	4	28.00	31.82	
Deterministic $(n=16)$	8	28.01	31.84	
Deterministic $(n=16)$	10	28.01	31.84	
Stochastic $(n=16)$	4	27.78	31.42	
Stochastic $(n=16)$	8	28.14	31.78	
Stochastic $(n=16)$	10	28.11	31.87	
Stochastic $(n=16)$	16	28.11	31.87	
Stochastic (n=16)	32	28.02	$\boldsymbol{31.92}$	

Table 6: Test BLEU scores of SUNDAE and Imputer (Saharia et al., 2020) distilled from AR Transformer–Base model on English-to-German (EN \rightarrow DE) and German-to-English (DE \rightarrow EN) translation tasks.

G SACREBLEU SCORES FOR WMT'14 EXPERIMENTS

SacreBLEU (Post, 2018) is a library for computing BLEU score⁷ that does not require the user to manually tokenize the reference and candidate translations. We report BLEU scores measured with SacreBLEU library in order to provide a reference for future studies. We show all the BLEU scores in Table 7.

		EN→DE		DE→EN		EN→FR	
Model	Steps (T)	BLEU	BLEU*	BLEU	BLEU*	BLEU	BLEU*
Deterministic $(n=16)$	2	20.29	20.13	25.28	24.83	31.60	30.51
Deterministic $(n=16)$	3	24.07	23.84	28.64	28.12	35.88	34.68
Deterministic $(n=16)$	4	25.01	24.75	29.53	28.99	36.85	35.61
Deterministic $(n=16)$	10	25.54	25.25	30.11	29.54	37.15	35.92
Stochastic $(n=16)$	4	23.05	22.75	28.13	27.62	35.27	34.03
Stochastic $(n=16)$	8	26.22	26.08	30.48	30.00	37.45	36.16
Stochastic $(n=16)$	10	26.25	25.99	30.80	30.24	27.53	36.23
Stochastic $(n=16)$	32	26.57	26.31	30.74	30.11	37.60	36.20

Table 7: Test BLEU without AR distillation (raw). Scores computed with SacreBLEU library are denoted as BLEU*.

H UNCONDITIONAL SAMPLES FOR C4

We provide samples for our model trained on C4 dataset as described in the main text (Section 3.2). All of them resemble reasonable-quality internet texts, except perhaps sample #4.

Index	Sample from our model
index	
1	I had to go back and forth and start over to see what had happened, what was working, and all the pieces were in the right places.
2	tossed in a delicious sauce.
2	Beef brisket is a hearty cut of meat – thick and tender. When you make a lot of meat
	can expect to see more of the same in 'Wild Herring', although not very often enough to achieve the same effect.
3	In 'Herring',
4	, she was considered to be a fake.
4	Dr. Deborah Chienna has 93 in the last 365 days., headaches, stomach pain, sore
	as an artist.
5	printing photo cards, artwork, and posters.
3	email me for some ideas.
	"Rebecca's studio
6	Jersey, Philadelphia and Washington DC. This is a conference attended by residents, physicians, graduate medical students, and others in the field of public health.
	's location.
7	This research was supported by a grant from the National Association for the Advancement of Science through the U.S. Department of Energy
	different artists, we would love to show you the piece we have in our shop!
8	Keep an eye on our Gallery – all you have to do is
	6.3 million from \$88.8 million reported by Zacks.com back in February.
9	Brad Brickley, general manager of Irvine, Califbased
10	to writing with the Autumns. Together, some of the class will spend time in the classroom to read a poem from the original book. From there we

Table 8: Unconditional samples from our model trained on C4 (without cherry-picking). Since C4 was crawled from the web, newline symbols are abundant both in the training data and the samples.

https://github.com/mjpost/sacrebleu

I UNCONDITIONAL SAMPLES FOR EMNLP2017 NEWS

We provide samples from our model trained on EMNLP2017 News dataset in Table 9, accompanying the quantitative results in the main text (Section 3.2). These samples are obtained at temperature 0.8. None of them appear in the training set, so the model does not merely memorize the data it is given. To provide a point of reference, we also include samples from ScratchGAN (d'Autume et al., 2019).

Index	Sample
ScratchGA	N
1	We are pleased for the trust and it was incredible, our job quickly learn the shape and get on that way.
2	But I obviously have him with the guys, maybe in Melbourne, the players that weren't quite clear there.
3	There is task now that the UK will make for the society to seek secure enough government budget fund reduce the economy.
4	Keith is also held in 2005 and Ted's a successful campaign spokeswoman for students and a young brothers has took an advantage of operator.
5	Police said how a Democratic police officer, would choose the honor of alcohol and reduce his defense and foundation.
6	We do not go the Blues because that I spent in ten months and so I didn't have a great job in a big revolution.
7	The 28 - year - old - son Dr Price said she would have been invited to Britain for her "friend" in a lovely family.
8	And as long as it is lower about, our families are coming from a friend of a family.
SUNDAE	
1	Ms Sturgeon was quoted as saying that she is prepared to quit the EU by the end of March next year.
2	They 've been around a long time, but it 's too natural to ignore what has happened.
3	"It's a busy road, and we've got to get through it," he said.
4	That means some voters will decide if they 'll change their minds before the first day of the debate.
5	"We don't learn very much from my point of view because we live here," he said.
6	"I spent my whole life at the stage and now I' m a normal father," he continued.
7	Whether your phone is near or online, you can check if your phone is tied to your Instagram account.
8	"It is only too early to know why the incident occurred shortly after it happened," he told the Associated Press.
9	The website will be updated on a day - to - day basis, as well as other special services.
10	So it 's too early to know exactly what each candidate has to say in terms of the American election.

Table 9: Unconditional samples from our model SUNDAE trained on EMNLP2017 News (without cherry-picking). We also provide samples from ScratchGAN (d'Autume et al., 2019) for comparison.

J PSEUDOCODE OF SUNDAE

We provide Python-like pseudocode for our method in Listing 1. The main functions are build_loss_fn, which should be used for training, and sampling_fn which should be used for sampling. For simplicity, we consider the decoder-only setup as in unconditional generation experiments (Section 3.2).

```
def get_random_text(shape, vocab_size):
    random_text = rand_int(shape, minval=0, maxval=vocab_size)
    return random_text
6 def corrupt_text(batched_text, vocab_size):
    corruption_prob_per_sequence = rand_uniform([batched_text.shape[0], 1])
    rand = rand_uniform(batched_text.shape)
    mask = rand < corruption_prob_per_sequence</pre>
    random_text = get_random_text(batched_text.shape, vocab_size)
10
    corrupted = mask * random_text + (1 - mask) * batched_text
11
    return corrupted
12
13
14
15 def build_logits_fn(vocab_size, n_unrolled_steps, enable_sampling):
16
    def logits_fn(batched_text):
17
      model = Transformer(vocab_size, use_causal_mask=False)
18
19
      def fn(input_batched_text):
20
        logits = model(input_batched_text)
22
        return logits
23
      def unrolled_fn(input_batched_text):
24
25
        samples = corrupt_text(input_batched_text, vocab_size)
26
        all_logits = []
        for _ in range(n_unrolled_steps):
27
```

```
logits = fn(samples)
28
          samples = stop_grad(rand_categorical(logits))
29
          all_logits += [logits]
30
        final_logits = concatenate(all_logits, axis=0)
31
        return final_logits
32
33
      if enable_sampling:
34
        return fn(batched_text)
35
36
37
        return unrolled_fn(batched_text)
38
39
    return logits_fn
40
41
42 def build_loss_fn(vocab_size, n_unrolled_steps=2):
    logits_fn = build_logits_fn(
43
        vocab_size, n_unrolled_steps, enable_sampling=False)
44
45
46
    def loss_fn(batched_text):
      logits = logits_fn(batched_text)
47
      # repeat batched_text to fit unrolled logits
48
49
      targets = concatenate([batched_text] * n_unrolled_steps, axis=0)
      one_hot_targets = one_hot(targets, vocab_size)
50
51
      loss_per_token = -sum(
          one_hot_targets * log_softmax(logits), axis=-1)
52
      loss = mean(loss_per_token)
53
      return loss
54
55
56
    return loss_fn
57
58
59 def sampling_fn(logits_fn, steps, temperature, batch_size,
60
                  sequence_length, vocab_size):
    batched_text = get_random_text(
61
       shape=[batch_size, sequence_length], vocab_size)
62
63
    for _ in range(steps):
64
      logits = logits_fn(batched_text)
      samples = rand_categorical(logits / temperature)
65
      batched_text = samples
66
  return batched_text
```

Listing 1: Pseudocode of SUNDAE.

K Longer unconditional samples for C4

This section shows Table 10 containing selected samples for our model trained on longer 256-token-length sequences of C4 dataset. The details of training are described in the main text (Section 3.2). For comparison, we also show unconditional samples from a recent discrete diffusion paper D3PM (Austin et al., 2021) modeling 128-token-length sequences of LM1B dataset (Chelba et al., 2013) in Table 11. While the dataset and the setup are different between the papers, this still gives us some hints as to how samples compare. SUNDAE qualitatively produces more globally coherent and grammatically correct samples than D3PM.

Index Sample from our model

land area of England that was suffering from a range of honey production problems. The effects of habitat degradation also led to a decline in tourism and a decrease in farming, probably leading to a decline in beekeeping. This development makes sense in reference to the UK's coastal area which never received environmental protection until the 1980s, when parts of England in the south and parts of the east coast were identified as a crisis zone.

The colonies in the UK collect surplus honey from the great ancient woodlands of England. Only 40% of these are left. In the 1970's, a study was conducted on "honey waste and recreation" in Germany and Austria. However, as a result of these studies, a method for processing was developed with the addition of sugar extraction. Using this method it is possible to render the rest of the honey with the commercially available sugar and to provide a certain stimulant and anti-tumor agent, for example, Radicolloid. As the sugar moves to moisture, the honey turns to fat to obtain the extent necessary for the improvement of product quality.

This method capitalizes on beekeeping which is a growing industry in the UK's woodland region. The honey is collected from the woodlands of the south of England

selling the house. To help with that, hire a real estate agent who can help you make an effort to sell a house that has been selling for over ten years.

Make sure that you properly tour the house and ensure that you will make the necessary repairs in an effort to sell the house. Take some time to take professional photos. These will be the things buyers will see and remember so that you can sell the house. An agent can help you prepare for a successful sale and the following tips can help you be prepared for a successful sale of the house and bring in more qualified buyers.

There is no restriction on the amount that you have to list. However, if a seller chooses not to list his house, he cannot list it above the original asking price. If you need to advertise things such as HOA, no worries, list less. A homebuyer can take advantage of a buyer willing to list for less to sell.

When you sell a house to a buyer, you should price it and then discuss it with the buyer so you can put out an offer. The more you have to offer, the higher the sale price will be. If you don't price it properly, it is a loss to the seller. A buyer

3 its rural roots. Insurance companies were functioning differently than usual. In addition, fiscal restraints on state budgets, limited access to capital, and its status as a center for interstate sales, mean the market has yet to witness significant growth and change.

It's the same scenario that had taken place in the US when people were starting to move to Florida. A growing number of foreign investors were in Argentina back in the early 90s and not long after that they saw the need for disability insurance coverage – a product largely unavailable in Argentina.

With both Casa Insurance and its American counterpart, local business was improving and Casa was ready to enter Argentina. Western competitors like Newcomers and HSG Insurance were also in the Buenos Aires market. And the coverage gap in the insurance industry was fast-growing. Casa insurance offers affordable coverage for people on both the fringes of the country and its borders.

Unlike American counterparts, La Frontera Abra De Avila offers a range of options to suit a variety of market conditions. They offer competitive products and focus on customer safety and customer satisfaction ratings. Generally they are concerned about price and customer trust. They are not like their competitors. They gain trust from customers by offering better coverage

4 Ask for what you need. Know that, more than anything, you know that they're there and will be right now to help you and help take that first step off the path that you've been bogged down.

One of my favourite things to learn about each new phase is that when you're making decisions in your life, it's really hard to prepare for them. I also learn that it's a relief from loneliness and how to do it without pressure. Home is a sacred place to enjoy a new journey and unexpected loveliness. Whether you're enjoying a meal with friends or watching a movie, friends and family come together to enable you to do what you want to do.

This stage really is just the beginning. It's almost like two parallel stages of discovery. For me right now, traveling and living are all part of my journey. Moving to a new environment is about discovering my roots. It's an adventure that's exciting. But traveling and living can be overwhelming to navigate right now. After a while, I know I'll embrace and assimilate life back home with grace and ease.

When I graduate, I'll be ready to embark on the next

5 the client's office to view their work

The client's work has been done using a variety of techniques, covering a variety of photographic styles.

I have always loved digital photography, but with the advent of digital cameras, I wanted it to be an ally to the viewer when viewing their work, so I began with a series of the original clip art photographs shot in film format. As means of manipulation, the photographer captured wide angle "off-camera" images, which are in close proximity to the camera. This technique allows the viewer to see what the photographer was able to capture off-camera and creates a more realistic image of the scene. In addition, the photographer moves the camera up, or up closer to the viewer, to light the series of photographs to create "faster" images.

The original clip art appears to retouch the image onto the film for display on the wall, however, in the digital medium, the image appears temporarily on the wall. The photographs were used as potential reminders for the client. The client selected this photograph as a memorial to the original clip art, along with the name of the photograph. With a little practice, it appeared the photograph was embedded in the clip art, and so

Table 10: Selected unconditional samples from our model trained on longer sequences of C4.

Index	Sample
1	The expected this year will be to bankroll private developers with a new program to develop nuclear energy . "Women , for example , could" use insulin how to use it and hide in detectable function , "said Michelle Ngum , president of the agency for the DWI Field techniques , who reported her research on what inspires women with DNA 's . MONIX INTO FEUR Jonny Pearlmunds is backup goalie . Coach Sedley "didn't respond to
2	Roman ("top") and Nazis frequently invade the United Nations . But some were questioning whether this joint action , though necessary , would have assailed their positions . The man on the orders of Franz Schnuecky is a Centacle lobbyist . Regardless , this season of success gives it something to make people spend money , but on Sundays the camera 's most popular spot may be responsible : ban hallouber with a buffalo companion that doesn 't even
3	assets . What will America see these plays into these underpockety? – Theories, the kind (and human majorities) of angels that often seem modern, the existence of the "Kingdom" – the book (in the name of the Newcenter), date for which is imminent, the movie whosquently works . "Lake Mart's real landscape is therefore very hearty because it's very important for many firemen to survive the storm," the newspaper reported
4	grateful, not being spy with plenty of boos. Mr. Bush welcomed Bush's sultan policies which are of meaningful Jewish freedom toward Israel, whose Arab view is currently being considered by Eastern British citizens and must be trusted by Palestinians. Second cost, $Club \pm 32$. If I were here to make an appointment and then think about breast cancer. He was totally a terrifi of caution. Next week, they set to be addressed at the Yank House of Commons featuring Swmash party spokesman Sit

Table 11: Unconditional samples from a recent discrete diffusion paper D3PM (Austin et al., 2021) modeling 128-token-length sequences of LM1B dataset (Chelba et al., 2013).